

Pontryagin-Guided Policy Optimization for Merton's Portfolio Problem

Jeonggyu Huh¹ and Jaegi Jeon^{*2}

¹Department of Mathematics, Sungkyunkwan University, Republic of Korea
²Graduate School of Data Science, Chonnam National University, Republic of Korea

January 14, 2025

Abstract

We present a Pontryagin-Guided Direct Policy Optimization (PG-DPO) framework for Merton's portfolio problem, unifying modern neural-network-based policy parameterization with the adjoint viewpoint from Pontryagin's maximum principle (PMP). Instead of approximating the value function (as done in deep BSDE methods), we track a policy-fixed BSDE for the adjoint processes, which allows each gradient update to align with continuous-time PMP conditions. This setup yields locally optimal consumption and investment policies that are closely tied to classical stochastic control. We further incorporate an alignment penalty that nudges the learned policy toward Pontryagin-derived solutions, enhancing both convergence speed and training stability. Numerical experiments confirm that PG-DPO effectively handles both consumption and investment, achieving strong performance and interpretability without requiring large offline datasets or model-free reinforcement learning.

1 Introduction

Merton's portfolio optimization problem (Merton, 1971) is a cornerstone of mathematical finance, aiming to specify optimal investment and consumption decisions in a continuous-time market. Classical treatments (e.g., Karatzas & Shreve, 1998; Yong & Zhou, 2012; Pham, 2009) exploit the problem's analytical tractability to

^{*}Corresponding Author: jaegijeon@jnu.ac.kr

derive closed-form solutions under specific assumptions, such as constant coefficients or complete markets. In real-world settings, however, these idealized conditions are often not met, prompting practitioners to rely on data-driven methods that do not assume closed-form solutions. By parameterizing the policy (both investment and consumption) with neural networks and defining a suitable objective, one can use gradient-based learning (e.g., stochastic gradient descent) to iteratively improve the policy. Such deep-learning-based approaches have shown promise for high-dimensional state spaces, path dependence, and market frictions (Han & E, 2016; Han et al., 2018; Beck et al., 2019; Buehler et al., 2019; Becker et al., 2019; Zhang & Zhou, 2019; Reppen et al., 2023; Reppen & Soner, 2023).

Despite these advances, a purely empirical or black-box gradient approach may overlook the continuous-time optimal control perspective. Without classical stochastic control principles as guidance, there is no clear guarantee that iterative updates will converge to a Pontryagin-aligned policy, that is, one satisfying the adjoint-based optimality conditions in continuous time. Recent studies (e.g., Reppen et al., 2023; Reppen & Soner, 2023) highlight this tension: while purely data-driven methods can achieve high performance in practice, they may not incorporate the deeper theoretical underpinnings of optimal control. Other works, such as Dai et al. (2023), adopt model-free reinforcement learning (RL), which requires extensive exploration and often omits consumption to focus on investment alone.

A different perspective is offered by the so-called deep BSDE (backward stochastic differential equation) methodology, pioneered by Weinan E and collaborators (e.g., Han et al., 2018; Weinan, 2017), which focuses on approximating the value function (i.e., solving the Hamilton-Jacobi-Bellman (HJB) equation) via a forward-backward stochastic differential equation (FBSDE), then infers the policy once the value function is estimated. By contrast, our approach is fundamentally adjoint-based: rather than approximating the value function, we track adjoint (costate) processes through a policy-fixed BSDE and use them to guide parameter updates directly. In addition, we implement this scheme via backpropagation-through-time (BPTT), unrolling the system dynamics in discrete steps and enabling single-path simulation for each node. While both deep BSDE and our Pontryagin-guided approach employ neural networks and stochastic differential equations (SDEs), the difference in what is learned (value function vs. adjoint) and how it is integrated (decoupled vs. direct BPTT) can yield distinct interpretability and computational trade-offs.

However, to the best of our knowledge, no existing deep-BSDE or physics-informed neural networks (PINNs) approach has tackled the Merton problem with both consumption and investment in a single framework. Most related works address either an investment-only Merton setup or simpler PDEs (e.g., Black-

Scholes) via PINNs (Han et al., 2018; Huré et al., 2020). This gap further motivates our approach, which integrates Pontryagin’s principle with a fully neural-network-based solver that jointly handles both consumption and investment.

Our framework adopts what we call a Pontryagin-Guided Direct Policy Optimization (PG-DPO) viewpoint. We treat the Merton problem as a continuous-time stochastic control system but solve it through direct neural-network-based optimization. Specifically, we embed Pontryagin’s Maximum Principle (PMP) (Pontryagin, 2018) into a discrete-time training loop, interpreting each gradient step as an approximation to the continuous-time adjoint. This preserves the convenience of automatic differentiation and mini-batch simulation while offering a principled control-theoretic justification of policy improvement. We also incorporate both consumption and investment into the policy, a combination seldom tackled simultaneously by purely data-driven methods yet crucial in real-world portfolio planning.

Our numerical experiments and theoretical analyses demonstrate that this direct policy optimization (DPO) (Reppen et al., 2023; Reppen & Soner, 2023) approach converges to stationary policies that are strongly aligned with Pontryagin’s conditions. Moreover, viewing the adjoint through the Pontryagin lens facilitates an alignment penalty (or regularization) that can speed up convergence. This additional penalty encourages the network’s consumption and investment policies to stay near Pontryagin-derived controls at each time instant, thereby improving training efficiency and stability in practice. In many cases, the policy converges to a local optimum that remains consistently Pontryagin-aligned and does so without relying on large offline datasets or purely model-free RL techniques.

Several aspects of this paper can be summarized as follows. First, we propose a PG-DPO scheme that incorporates PMP in a discrete-time neural network framework. Each gradient update is interpreted in terms of the adjoint perspective, providing a more transparent route to near-optimal solutions than opaque gradient-based updates alone. Second, we add an adjoint-based alignment penalty, encouraging the neural policy to stay close to locally Pontryagin-optimal controls and thereby taking advantage of suboptimal adjoint estimates for faster convergence. Although we only guarantee local optimality, this soft constraint often yields notable improvements in training efficiency and stability. Third, by directly tackling both consumption and investment in the Merton problem, we address a more challenging scenario than usual in data-driven approaches. Our method converges reliably, uses rolling simulations (thus mitigating overfitting), and handles the entire state-time domain with a single pipeline. Finally, the Pontryagin viewpoint supports interpretability by making the adjoint processes explicit, while still preserving the flexibility of modern deep-learning tools. This synergy can naturally extend to more general setups involving jumps, constraints, or multi-asset

portfolios.

Section 2 reviews the continuous-time Merton formulation, emphasizing the interplay of consumption and investment. Section 3 revisits PMP and re-expresses Merton’s SDE via a forward-backward viewpoint, setting the stage for our adjoint-based approach. In Section 4, we contrast our method with deep BSDE frameworks that approximate the value function instead of the adjoint. Next, Section 5 explains the discrete-time updates that approximate the continuous-time Pontryagin flow, including an alignment penalty for faster convergence. In Section 6, we use a stochastic approximation viewpoint (Robbins-Monro theory) to show that our method converges locally. Section 7 presents numerical experiments demonstrating convergence to robust local optima aligned with Pontryagin’s conditions. Finally, Section 8 offers concluding remarks and discusses possible extensions that further bridge deep learning and stochastic control.

2 Continuous-Time Formulation of the Merton Portfolio Problem

We focus on Merton’s portfolio optimization problem, in which an investor allocates wealth between a risky asset S_t and a risk-free asset B_t . The risky asset follows a geometric Brownian motion:

$$dS_t = \mu S_t dt + \sigma S_t dW_t,$$

where W_t is the standard Brownian motion, and the risk-free asset evolves as

$$dB_t = rB_t dt.$$

Let X_t denote the investor’s total wealth at time t . The investor continuously consumes at rate C_t and invests proportion π_t of X_t in the risky asset, so that X_t satisfies

$$dX_t = (rX_t + \pi_t(\mu - r)X_t - C_t) dt + \pi_t\sigma X_t dW_t, \quad X_0 = x_0 > 0. \quad (1)$$

We consider the objective function:

$$J(\pi_t, C_t) := \mathbb{E} \left[\int_0^T e^{-\rho t} U(C_t) dt + \kappa e^{-\rho T} U(X_T) \right], \quad (2)$$

where

$$U(x) = \frac{x^{1-\gamma}}{1-\gamma} \quad (3)$$

is a CRRA (constant relative risk aversion) utility function, $\rho > 0$ is a discount factor, and $\kappa > 0$ is a parameter that modulates the relative weight of terminal wealth (bequest). We parametrize the investment and consumption via neural networks:

$$\pi_t = \pi_\theta(t, X_t), \quad C_t = C_\phi(t, X_t),$$

where θ and ϕ denote the network parameters to be learned.

In a continuous-time stochastic control framework, these controls $\{\pi_t, C_t\}$ must be admissible. Concretely, this means each π_t and C_t must be adapted and measurable with respect to the filtration generated by $\{W_t\}$, thereby depending only on information available up to time t . They also require boundedness or controlled growth (e.g. $|\pi_t| \leq M_\pi$, $C_t \geq 0$) to prevent explosive behavior in the state dynamics and ensure the integrals in the objective function (2) remain finite. Moreover, the choices of $\{\pi_t, C_t\}$ should preserve the nonnegativity of the wealth process X_t almost surely. Under these conditions, the SDE governing X_t admits a unique strong solution, and the objective $J(\pi_t, C_t)$ is well-defined. In practice, one can fulfill these feasibility constraints by selecting suitable activation functions or output layers in the neural networks π_θ and C_ϕ , ensuring that every sampled trajectory respects the required conditions automatically.

A key property of the Merton problem is the strict concavity of the CRRA utility (3). This strict concavity guarantees the uniqueness of the global maximum and motivates classical results (Merton, 1971; Karatzas & Shreve, 1998; Yong & Zhou, 2012) indicating that any stationary point of $J(\pi_t, C_t)$ is, in fact, the unique global maximizer. This uniqueness is central to the theoretical analysis we develop.

In the classical Merton problem with CRRA utility and no bequest ($\kappa = 0$), closed-form solutions are well-known. For example, in the infinite-horizon setting with discount rate $\rho > 0$, the optimal investment and consumption rules reduce to constant values:

$$\pi_t^* = \frac{\mu - r}{\gamma\sigma^2}, \quad C_t^* = \nu X_t, \quad \text{where } \nu = \frac{\rho - (1 - \gamma) \left(\frac{(\mu - r)^2}{2\sigma^2\gamma} + r \right)}{\gamma}. \quad (4)$$

This form shows that a constant fraction of wealth is invested in the risky asset, and consumption is proportional to current wealth at a constant rate ν .

In more general settings, such as a finite time horizon T or when the bequest term $\kappa > 0$ is included, the closed-form solutions become slightly more involved but remain explicit. For instance, under a finite horizon T and $\kappa > 0$, the optimal consumption satisfies

$$C_t^* = \nu \left(1 + (\nu\epsilon - 1) e^{-\nu(T-t)} \right)^{-1} X_t, \quad \text{where } \epsilon = \kappa^{1/\gamma}$$

and ν is the same constant defined in (4). As $T \rightarrow \infty$, this expression converges to the infinite-horizon solution in (4). These analytical formulas serve as exact

solutions that confirm our neural network-based policy indeed converges to the theoretically optimal strategy. We shall use these formulas in Section 7 as a numerical reference.

3 Pontryagin’s Maximum Principle and Its Application to Merton’s Problem

3.1 Pontryagin’s Maximum Principle

PMP provides necessary conditions for optimality in a broad class of continuous-time stochastic control problems (see, e.g., Pontryagin, 2018; Pardoux & Peng, 1990; Fleming & Soner, 2006; Yong & Zhou, 2012; Pham, 2009). To illustrate this principle in a general setting, consider a system whose state X_t evolves according to the SDE

$$dX_t = b(t, X_t, u_t) dt + \sigma(t, X_t, u_t) dW_t, \quad X_0 = x_0, \quad (5)$$

where u_t is an admissible control. The goal is to maximize an objective functional of the form

$$J(u) = \mathbb{E} \left[\int_0^T g(t, X_t, u_t) dt + G(X_T) \right].$$

If there exists an optimal control u_t^* that attains the supremum of $J(u)$, we denote by J^* the corresponding optimal value function. PMP is invoked by constructing a Hamiltonian

$$\mathcal{H}(t, X_t, u_t, \lambda_t, Z_t) = g(t, X_t, u_t) + \lambda_t b(t, X_t, u_t) + Z_t \sigma(t, X_t, u_t),$$

along with adjoint (costate) processes λ_t and Z_t . Under the optimal control u_t^* , the state process X_t^* is simply the unique solution of the original SDE (5), where (X_t, u_t) is replaced by (X_t^*, u_t^*) . Formally,

$$dX_t^* = b(t, X_t^*, u_t^*) dt + \sigma(t, X_t^*, u_t^*) dW_t, \quad X_0^* = x_0. \quad (6)$$

In this setting, the adjoint λ_t^* can be viewed as $\lambda_t^* = \frac{\partial J^*}{\partial X_t}$, capturing how marginal changes in X_t affect the optimal value. In turn, (λ_t^*, Z_t^*) satisfies a BSDE

$$d\lambda_t^* = -\frac{\partial \mathcal{H}}{\partial X}(t, X_t^*, u_t^*, \lambda_t^*, Z_t^*) dt + Z_t^* dW_t, \quad \lambda_T^* = \frac{\partial G}{\partial X}(X_T^*). \quad (7)$$

Solving the BSDE (7) together with the forward SDE (6) for X_t^* forms a coupled FBSDE system. From this system, one obtains not only the optimal state

trajectory X_t^* and the adjoint processes (λ_t^*, Z_t^*) , but also characterizes the optimal control u_t^* by maximizing the Hamiltonian with respect to u at each time t . Through this local maximization step, PMP effectively transforms the global control problem into a condition that must hold pointwise in time.

As a result, it offers a systematic way to compute (or approximate) the optimal control, unifying value sensitivities λ_t^* , noise sensitivities Z_t^* , and the evolving state X_t^* in one mathematical framework (Fleming & Soner, 2006; Yong & Zhou, 2012; Pham, 2009). In the sections that follow, we will see how this general procedure applies specifically to the Merton portfolio problem, illustrating how adjoint processes guide both investment and consumption decisions in a continuous-time setting.

3.2 Pontryagin Adjoint Processes and Parameter Gradients in the Merton Problem

In this subsection, we combine two key components for handling both the optimal Merton problem and suboptimal parameterized policies. First, we restate the Pontryagin conditions for the Merton setup, which yield the optimal relationships among $(\lambda_t^*, Z_t^*, \pi_t^*, C_t^*)$. Second, we explain how to generalize these adjoint processes to a policy-fixed BSDE in the suboptimal setting and derive corresponding parameter gradients.

3.2.1 Pontryagin Formulation for Merton's Problem

Recall that in the Merton problem, we aim to maximize

$$J(\pi_t, C_t) = \mathbb{E} \left[\int_0^T e^{-\rho t} U(C_t) dt + \kappa e^{-\rho T} U(X_T) \right],$$

subject to

$$dX_t = (rX_t + \pi_t(\mu - r)X_t - C_t) dt + \pi_t \sigma X_t dW_t, \quad X_0 = x_0 > 0$$

where $U(\cdot)$ is a CRRA utility function, $\rho > 0$ is a discount rate, and $\kappa > 0$ represents the bequest weight. To apply PMP in this setting, we define the Hamiltonian

$$\mathcal{H}(t, X_t, \pi_t, C_t, \lambda_t, Z_t) = e^{-\rho t} U(C_t) + \lambda_t [rX_t + (\mu - r)\pi_t X_t - C_t] + Z_t \pi_t \sigma X_t.$$

From PMP, the optimal controls (π_t^*, C_t^*) maximize \mathcal{H} pointwise in (π_t, C_t) . Differentiating with respect to C_t and π_t and setting these partial derivatives to zero yields:

(a) **Consumption:**

$$\frac{\partial \mathcal{H}}{\partial C_t} = e^{-\rho t} U'(C_t^*) - \lambda_t = 0 \implies U'(C_t^*) = e^{\rho t} \lambda_t^*.$$

Since $U'(x) = x^{-\gamma}$, it follows that

$$C_t^* = \left(e^{\rho t} \lambda_t^* \right)^{-\frac{1}{\gamma}}. \quad (8)$$

(b) **Investment:**

$$\frac{\partial \mathcal{H}}{\partial \pi_t} = (\mu - r) \lambda_t^* X_t^* + Z_t^* \sigma X_t^* = 0 \implies (\mu - r) \lambda_t^* + \sigma Z_t^* = 0.$$

Thus, the optimal adjoint processes satisfy $Z_t^* = -\frac{(\mu-r)}{\sigma} \lambda_t^*$.

Hence, the pair (λ_t^*, Z_t^*) links directly to the optimal controls (π_t^*, C_t^*) . In practice, λ_t^* can be interpreted as the sensitivity of the optimal cost-to-go with respect to the state X_t , while Z_t^* captures the sensitivity to noise.

Remark (Expressing π_t^* in terms of λ_t^* and Z_t^* under regularity). In many one-dimensional settings, including the Merton problem, an additional smoothness assumption on the FBSDE system leads to the relation

$$Z_t^* = (\partial_x \lambda_t^*) \sigma \pi_t^* X_t^*,$$

where $\partial_x \lambda_t^*$ denotes the spatial derivative of λ_t^* with respect to the wealth variable x . Dividing both sides by λ_t^* and using $(\mu - r) \lambda_t^* + \sigma Z_t^* = 0$, we obtain

$$-\frac{\mu - r}{\sigma} = \frac{Z_t^*}{\lambda_t^*} = \frac{\partial_x \lambda_t^*}{\lambda_t^*} \sigma \pi_t^* X_t^*.$$

Hence, under suitable conditions (e.g., if $\partial_x \lambda_t^* / \lambda_t^*$ remains bounded and nondegenerate), one can solve for π_t^* explicitly:

$$\pi_t^* = \frac{\mu - r}{\sigma^2} \times \frac{-\lambda_t^*}{\partial_x \lambda_t^*} \frac{1}{X_t^*}. \quad (9)$$

In the classical Merton problem with CRRA utility (3), solving the entire forward-backward system reveals that $\partial_x \lambda_t^*$ is proportional to λ_t^* . Equivalently, the ratio

$$\frac{-\partial_x \lambda_t^*}{\lambda_t^*} X_t^* = \gamma$$

becomes a constant in both time and wealth. This reflects the well-known fact that CRRA utility fixes the investor’s relative risk aversion to γ , thereby forcing π_t^* to be a constant fraction of wealth:

$$\pi_t^* = \frac{\mu - r}{\gamma\sigma^2}.$$

But more generally, even if π_t^* depends on time or wealth in a nontrivial way, the above relationship shows how one can characterize it through the ratio $\frac{Z_t^*}{\lambda_t^*}$ (and partial derivatives of λ_t^*), once the full forward–backward system is solved.

3.2.2 Policy-Fixed Adjoint Processes for Suboptimal Policies

In classical PMP theory, the adjoint processes λ_t^* and Z_t^* naturally emerge from the FBSDE system associated with the optimal policy that maximizes the Hamiltonian. However, one can extend these adjoint processes to suboptimal policies as well. This extended notion is often called the policy-fixed adjoint, because the policy is treated as given (hence, fixed) rather than being chosen to maximize \mathcal{H} in each infinitesimal step.

Suppose we have a parameterized, potentially suboptimal policy (π_t, C_t) that does not necessarily satisfy the first-order optimality conditions. We can still define a Hamiltonian \mathcal{H} with the terminal cost $G(X_T)$, which might be, for instance, $\kappa e^{-\rho T} U(X_T)$ as in the Merton problem.

Although (π_t, C_t) is not chosen to maximize \mathcal{H} , we may formally differentiate \mathcal{H} with respect to the state X and postulate a BSDE for λ_t and Z_t :

$$d\lambda_t = -\frac{\partial \mathcal{H}}{\partial X}(t, X_t, \pi_t, C_t, \lambda_t, Z_t) dt + Z_t dW_t, \quad \lambda_T = \frac{\partial G}{\partial X}(X_T). \quad (10)$$

Since the policy (π_t, C_t) does not maximize \mathcal{H} , these adjoint processes λ_t and Z_t do not encode the standard PMP optimal costate condition. Instead, they represent the local sensitivities of the resulting objective $J(\pi_t, C_t)$ with respect to changes in the state X_t under the current suboptimal policy. For this reason, one often refers to them as “suboptimal” or “policy-fixed” adjoint processes. A comparison between the optimal policy case and the suboptimal policy case is as follows:

- (a) **Optimal Policy Case:** If (π_t^*, C_t^*) actually maximizes \mathcal{H} at each instant, then (λ_t^*, Z_t^*) coincide with the usual PMP adjoint processes, satisfying $\frac{\partial \mathcal{H}}{\partial \pi} = 0$, $\frac{\partial \mathcal{H}}{\partial C} = 0$, etc.
- (b) **Suboptimal Policy Case:** Here, $\frac{\partial \mathcal{H}}{\partial \pi} \neq 0$ or $\frac{\partial \mathcal{H}}{\partial C} \neq 0$, so (λ_t, Z_t) do not necessarily satisfy the typical PMP coupled conditions. Nonetheless, the

BSDE (10) remains well-defined under standard Lipschitz and integrability assumptions, thus clarifying how “the current policy plus small perturbations in X_t ” affects the cost functional. This perspective will be crucial in the gradient-based updates for suboptimal (parameterized) policies, discussed in the next sections.

3.2.3 Iterative Policy Improvement

Recall from Section 2 that we parametrize the investment and consumption controls as neural networks, $\pi_\theta(t, X_t)$ and $C_\phi(t, X_t)$, where (θ, ϕ) collect all network parameters. By these definitions, the overall performance $J(\theta, \phi)$, introduced in (2), depends on (θ, ϕ) through the drift and diffusion of X_t , as well as through direct utility terms involving C_ϕ . A central observation is that each small change in (θ, ϕ) —through these neural-network-based controls $\pi_\theta(t, X_t)$ and $C_\phi(t, X_t)$ —affects the drift and diffusion of X_t and thus the overall performance $J(\theta, \phi)$. To capture this dependence efficiently, one introduces a pair (λ_t, Z_t) via a BSDE (often called the “policy-fixed adjoint”), where λ_t acts much like $\frac{\partial J}{\partial X_t}$ and Z_t encodes sensitivity to noise.

As described in (1), the state process X_t (total wealth) can be rewritten as

$$dX_t = b(X_t; \theta, \phi) dt + \sigma(X_t; \theta, \phi) dW_t,$$

where

$$\begin{aligned} b(X_t; \theta, \phi) &= rX_t + \pi_\theta(t, X_t) (\mu - r) X_t - C_\phi(t, X_t), \\ \sigma(X_t; \theta, \phi) &= \sigma\pi_\theta(t, X_t) X_t. \end{aligned} \tag{11}$$

Gradient with respect to θ . When we differentiate b and σ in (11) with respect to θ , only the terms involving π_θ matter (since C_ϕ does not depend on θ). Concretely,

$$\begin{aligned} \frac{\partial}{\partial \theta} b(X_t; \theta, \phi) &= (\mu - r) X_t \frac{\partial \pi_\theta(t, X_t)}{\partial \theta}, \\ \frac{\partial}{\partial \theta} \sigma(X_t; \theta, \phi) &= \sigma X_t \frac{\partial \pi_\theta(t, X_t)}{\partial \theta}. \end{aligned} \tag{12}$$

Hence, if π_θ is implemented as a neural network, these partial derivatives reflect the network’s internal chain rule with respect to θ .

Next, recall that $\lambda_t = \frac{\partial J}{\partial X_t}$ and Z_t encodes noise sensitivity. By a standard chain rule argument in stochastic control, one obtains the general formula

$$\frac{\partial J}{\partial \theta} = \mathbb{E} \left[\int_0^T \left(\lambda_t \frac{\partial b}{\partial \theta} + Z_t \frac{\partial \sigma}{\partial \theta} \right) dt \right] + (\text{direct payoff dependence on } \theta), \tag{13}$$

where the “direct payoff” term collects any explicit dependence of the utility or terminal cost on θ . However, in many Merton-like settings, neither $U(\cdot)$ nor X_T

depends directly on θ (they depend on θ only through π_θ), so that term vanishes. Substituting $\frac{\partial b}{\partial \theta}$ and $\frac{\partial \sigma}{\partial \theta}$ from (12) yields

$$\begin{aligned}\frac{\partial J}{\partial \theta} &= \mathbb{E} \left[\int_0^T \left(\lambda_t (\mu - r) X_t \frac{\partial \pi_\theta}{\partial \theta} + Z_t \sigma X_t \frac{\partial \pi_\theta}{\partial \theta} \right) dt \right] \\ &= \mathbb{E} \left[\int_0^T (\lambda_t (\mu - r) X_t + Z_t \sigma X_t) \frac{\partial \pi_\theta}{\partial \theta} dt \right].\end{aligned}$$

Gradient with respect to ϕ . First, let us revisit the state-dynamics perspective. From (11), we have

$$\frac{\partial b}{\partial \phi} = -\frac{\partial C_\phi(t, X_t)}{\partial \phi}, \quad \frac{\partial \sigma}{\partial \phi} = 0.$$

Next, from the payoff perspective, $U(C_\phi(t, X_t))$ directly depends on ϕ , so it contributes an extra term $e^{-\rho t} U'(C_\phi(t, X_t)) \frac{\partial C_\phi}{\partial \phi}$. Combining these,

$$\begin{aligned}\frac{\partial J}{\partial \phi} &= \mathbb{E} \left[\underbrace{\int_0^T \lambda_t \left(-\frac{\partial C_\phi}{\partial \phi} \right) dt}_{\text{drift contribution}} \right] + \mathbb{E} \left[\underbrace{\int_0^T e^{-\rho t} U'(C_\phi(t, X_t)) \frac{\partial C_\phi}{\partial \phi} dt}_{\text{direct payoff contribution}} \right] \\ &= \mathbb{E} \left[\int_0^T \left(-\lambda_t + e^{-\rho t} e^{-\rho t} U'(C_\phi(t, X_t)) \right) \frac{\partial C_\phi(t, X_t)}{\partial \phi} dt \right].\end{aligned}$$

In words, $-\lambda_t \frac{\partial C_\phi}{\partial \phi}$ represents how C_ϕ reduces the drift in X_t (i.e. consumption lowers wealth), while $e^{-\rho t} U'(C_\phi) \frac{\partial C_\phi}{\partial \phi}$ captures the direct impact on running utility from changing consumption.

Deriving (13) via the Chain Rule. To see why (13) holds, recall that $J(\theta, \phi)$ depends on θ indirectly through the state process $X_t(\theta)$:

$$J(\theta, \phi) = \mathbb{E} \left[\int_0^T g(t, X_t(\theta), C_\phi(t, X_t)) dt + G(X_T(\theta)) \right],$$

where g and G represent the running cost and the terminal cost, respectively. By the chain rule, we can conceptually write

$$\frac{\partial J}{\partial \theta} = \mathbb{E} \left[\int_0^T \underbrace{\frac{\partial J}{\partial X_t}}_{\text{local sensitivity}} \frac{\partial X_t}{\partial \theta} dt \right] + \text{(possible direct dependence of } g, G \text{ on } \theta).$$

Here, $\frac{\partial J}{\partial X_t}$ captures how small fluctuations in X_t shift the overall performance, while $\frac{\partial X_t}{\partial \theta}$ describes how X_t itself is altered when θ changes.

Since we define $\lambda_t = \frac{\partial J}{\partial X_t}$ and Z_t for noise directions through a BSDE, each infinitesimal change in θ influences X_t via the drift b and diffusion σ , i.e.

$$\frac{\partial X_t}{\partial \theta} \mapsto \frac{\partial}{\partial \theta} b(\dots), \quad \frac{\partial}{\partial \theta} \sigma(\dots).$$

Hence, substituting $\lambda_t = \frac{\partial J}{\partial X_t}$ and unrolling the chain rule leads precisely to

$$\frac{\partial J}{\partial \theta} = \mathbb{E} \left[\int_0^T \left(\lambda_t \frac{\partial b}{\partial \theta} + Z_t \frac{\partial \sigma}{\partial \theta} \right) dt \right] + (\text{direct payoff dependence on } \theta), \quad (14)$$

where any running or terminal payoff that explicitly depends on θ (beyond b and σ) is grouped into the direct payoff term.

In a Merton-like setting, one often finds that θ enters J only via drift/diffusion, so this direct-payoff term vanishes. In more general problems, however, θ might appear explicitly in the payoff as well, adding another summand to (13).

For readers interested in a more rigorous derivation of the chain rule in stochastic settings (including variation of SDEs and the full FBSDE theory), we refer to classical treatments such as (Yong & Zhou, 2012; Ma & Yong, 1999; Pardoux & Peng, 1990). These works provide a comprehensive account of how one rigorously defines $\frac{\partial X_t}{\partial \theta}$ in a stochastic calculus framework and how the BSDE for (λ_t, Z_t) captures the costate processes in PMP.

4 Comparison with Deep BSDE Methods

In this section, we compare the adjoint-based BSDE approach from our Pontryagin framework with the value-based BSDE used in deep BSDE methods (e.g., Weinan, 2017; Han et al., 2018; Huré et al., 2020). Both lines of work exploit backward equations with neural network function approximators, but they differ fundamentally in their targets: our approach focuses on an adjoint process linked to PMP while deep BSDE aims at a value function typically derived from a PDE viewpoint.

4.1 Value-Based Methods (Deep BSDE)

4.1.1 Hamilton–Jacobi–Bellman Equation and the Value Function

Consider a controlled diffusion process:

$$dX_t = b(t, X_t, \alpha_t) dt + \sigma(t, X_t, \alpha_t) dW_t, \quad X_0 = x_0, \quad t \in [0, T], \quad (15)$$

where α_t is an admissible control. In a dynamic programming framework, the optimal value function $V^*(t, x)$ is defined as

$$V^*(t, x) = \sup_{\{\alpha_s: s \in [t, T]\}} \mathbb{E} \left[\int_t^T f(s, X_s, \alpha_s) ds + g(X_T) \mid X_t = x \right],$$

where f is a running reward (or negative cost) and g is a terminal reward. Under suitable smoothness assumptions, V^* satisfies a HJB equation:

$$\begin{aligned} -\frac{\partial V^*}{\partial t}(t, x) - \sup_{\alpha} \{ \mathcal{L}^{\alpha} V^*(t, x) + f(t, x, \alpha) \} &= 0, \\ V^*(T, x) &= g(x), \end{aligned} \tag{16}$$

where \mathcal{L}^{α} is the second-order differential operator associated with the SDE (15). Specifically,

$$\mathcal{L}^{\alpha} V = b(t, x, \alpha) V'(x) + \frac{1}{2} \sigma^2(t, x, \alpha) V''(x).$$

Once $V^*(t, x)$ is known, the optimal control $\alpha^*(t)$ is recovered pointwise by maximizing the Hamiltonian in (16), i.e.,

$$\alpha^*(t, x) = \arg \max_{\alpha} \{ \mathcal{L}^{\alpha} V^*(t, x) + f(t, x, \alpha) \}.$$

4.1.2 Deep BSDE Formulation

Rather than discretizing (16) directly, deep BSDE methods re-express the PDE solution through a FBSDE. In many cases, one may write a BSDE:

$$\begin{aligned} dY_t &= -f(t, X_t, \alpha_t, Y_t, Z_t) dt + Z_t dW_t, \\ Y_T &= g(X_T), \end{aligned} \tag{17}$$

where Y_t can be interpreted as $V^{\alpha}(t, X_t)$, the cost-to-go under the control α . If $\alpha_t = \alpha_t^*$ is the optimal control at every time t , then $V^{\alpha}(t, x)$ coincides with the optimal value function $V^*(t, x)$ from (16), and solving (17) recovers the same Y_t as the PDE solution $V^*(t, X_t)$. When α is suboptimal, (17) still holds as a representation of the suboptimal cost, but not of the true HJB value function.

In a deep BSDE approach, one typically parameterizes (Y_t, Z_t) via neural networks (Y^{θ}, Z^{θ}) and simulates forward the state X_t while integrating backward the pair (Y_t, Z_t) . Concretely, if θ collects all network parameters, one might write

$$Y_{t_k}^{\theta} = Y^{\theta}(t_k, X_{t_k}), \quad Z_{t_k}^{\theta} = Z^{\theta}(t_k, X_{t_k}),$$

and discretize (17) (e.g., via Euler-Maruyama). To train, one minimizes a loss function measuring consistency between these neural-network-based processes $(Y_{t_k}^{\theta}, Z_{t_k}^{\theta})$

and the BSDE dynamics. For instance, a mean-square error capturing the difference

$$Y_{t_k}^\theta - \left(Y_{t_{k+1}}^\theta + f(t_k, X_{t_k}, \alpha_{t_k}, Y_{t_k}^\theta, Z_{t_k}^\theta) \Delta t - Z_{t_k}^\theta \Delta W_k \right)$$

is computed over sampled paths $\{X_{t_k}\}$, along with the terminal condition error $|Y_{t_N}^\theta - g(X_{t_N})|^2$. By iterating gradient-based updates on θ , one obtains Y_t^θ that approximates $V^\alpha(t, X_t)$ under the chosen control sequence $\{\alpha_t\}$.

If α_t is known to be optimal (e.g., from an external iteration, or if α^* is given), then $Y_t^\theta \approx V^*(t, X_t)$. In that scenario, one can extract α_t^* by substituting V^* into the HJB equation (or Hamiltonian) and choosing α^* to maximize $\mathcal{L}^\alpha V^* + f(t, x, \alpha)$ at each point. Consequently, (17) directly encodes the value function rather than the control itself, so the policy is recovered only after one has identified or approximated the correct α^* .

4.2 Adjoint-Based Methods (Pontryagin's Principle)

Our approach bypasses the need to solve the full value function $V(t, x)$ and instead applies PMP directly. In classical PMP theory (Pontryagin, 2018; Fleming & Soner, 2006), the optimal control α_t^{*1} is obtained by maximizing a local Hamiltonian $\mathcal{H}(t, X_t, \alpha, \lambda_t^*, Z_t^*)$, thereby introducing a BSDE for the optimal adjoint (λ_t^*, Z_t^*) . Concretely, if we denote the terminal cost by $G(X_T)$, then

$$d\lambda_t^* = -\partial_x \mathcal{H}(t, X_t^*, \alpha_t^*, \lambda_t^*, Z_t^*) dt + Z_t^* dW_t, \quad \lambda_T^* = \partial_x G(X_T^*),$$

with

$$\alpha_t^* = \arg \max_{\alpha} \mathcal{H}(t, X_t^*, \alpha, \lambda_t^*, Z_t^*).$$

Here, $\lambda_t^* = \frac{\partial J^*}{\partial X_t}$ measures how changes in the state X_t affect the optimal cost J^* , while Z_t^* represents noise sensitivity. Substituting α_t^* back into \mathcal{H} at each time t yields the fully optimal feedback law in the continuous-time limit.

When $\alpha_t \neq \alpha_t^*$, one can define a so-called policy-fixed (suboptimal) BSDE by inserting the suboptimal control α_t into \mathcal{H} . This produces

$$d\lambda_t = -\partial_x \mathcal{H}(t, X_t, \alpha_t, \lambda_t, Z_t) dt + Z_t dW_t, \quad \lambda_T = \partial_x G(X_T),$$

where (λ_t, Z_t) now encode how the chosen (suboptimal) policy α_t influences the costate. Although λ_t here is not the fully optimal costate, it provides a local sensitivity framework similar to a policy-fixed BSDE in value-based methods. Iteratively adjusting α_t based on such suboptimal adjoint information can push α_t toward α_t^* , as long as the updates move in a direction that improves the global objective J .

¹In the Merton problem, this corresponds to $\alpha_t^* = (\pi_t^*, C_t^*)$.

In practice, we parameterize the control as $\alpha_\theta(t, X_t)$ with neural-network parameters θ , and define an overall objective $J(\theta)$ capturing the expected payoff (or negative cost). By computing $\nabla_\theta J(\theta)$ via BPTT and using the adjoint (λ_t, Z_t) under the current α_θ , we can perform gradient-based updates that locally maximize J . Repeating these updates refines α_θ until it approaches to the optimal α_t^* . Correspondingly, the costate (λ_t, Z_t) approaches to (λ_t^*, Z_t^*) , maintaining a consistent PMP-based BSDE perspective throughout.

In summary, deep BSDE methods approximate the value function by solving an HJB equation or a BSDE for $V(t, x)$, then infer the policy afterwards. By contrast, Pontryagin-adjoint approaches solve a different BSDE for the costate (λ_t, Z_t) and directly update the policy at each iteration. These perspectives involve distinct computational trade-offs:

- Deep BSDE can be advantageous if one explicitly needs value function $V(t, x)$ across the entire domain or must solve high-dimensional PDEs where direct HJB methods are infeasible.
- Pontryagin-adjoint can offer a more streamlined route to an optimal policy, particularly when multiple controls must be determined (e.g., consumption and investment in the Merton problem), where extracting each control from a single value function might prove cumbersome in a value-based approach.

Overall, one's choice between these methods depends on whether the value function itself is the main quantity of interest, or whether they prefer a more direct, adjoint-based path to optimizing the policy.

5 Gradient-Based Algorithm for Stationary Point Convergence

In the previous sections, we showed how PMP yields adjoint processes (λ_t, Z_t) that guide control optimization in continuous time. Here, we focus on the practical implementation side: specifically, how to design a neural-network-based scheme that leverages these adjoints (or their estimates) to learn an approximately optimal policy for the Merton problem. We embed the PMP conditions into a discrete-time training procedure, thereby uniting classical control theory with modern deep learning frameworks.

Our approach relies on BPTT over a discretized version of the stochastic system. By treating (λ_t, Z_t) as suboptimal adjoint processes associated with the current parameterized policy, each gradient update moves the policy closer to a Pontryagin-aligned solution. Additionally, we introduce a regularization, which

we call an “alignment penalty”, to encourage consumption and investment decisions to stay near the locally optimal Pontryagin controls at each node. This soft enforcement can reduce variance, accelerate convergence, and stabilize training.

The remainder of this section is organized as follows:

- Section 5.1 revisits the single-path approach for estimating λ_t and Z_t at each time-state point (t, x) . Although each single sample can be high variance, it remains an unbiased estimator and underpins the rest of our method.
- Section 5.2 presents a concrete, discrete-time algorithm for computing $\nabla_{\theta} J$ and $\nabla_{\phi} J$. We then perform standard gradient steps to update the policy networks, leveraging the sampled adjoint information.
- Section 5.3 explains how to include an alignment penalty that softly enforces consistency between the learned policy and the Pontryagin-derived controls $(\pi^{\text{PMP}}, C^{\text{PMP}})$ at each node.
- Section 5.4.1 extends our perspective to a global-in-time, extended value function setup that handles any initial node (t_0, x_0) , crucial for covering a broad domain. We then detail two Pontryagin-Guided DPO algorithmic variants in Section 5.4.2.

Overall, we show that by embedding PMP within a BPTT-based stochastic gradient framework, one can converge rapidly to a near-optimal strategy in Merton’s problem while retaining the flexibility and scalability of neural networks.

5.1 Single-Path Approach for Each (t, x)

A central insight of our method is that a single forward simulation (or single path) can produce an unbiased estimate of the adjoint processes (λ_t, Z_t) for a given (t, x) . Specifically, $\lambda_t = \partial J / \partial X_t$ measures how changes in the state X_t affect the cost J . In one-dimensional problems like Merton’s, we also have

$$Z_t = \sigma \pi_t X_t (\partial_x \lambda_t). \quad (18)$$

Using just one forward path for each node (t_k, X_k) is attractive for several reasons. First, although each single path is noisy, the average over many such paths converges to the true adjoint in expectation (Kushner & Yin, 2003; Borkar & Borkar, 2008). Second, minimal overhead is required per sample, because we do not store or simulate large ensembles for the same node; each node simply spawns exactly one forward simulation. Third, this setup naturally supports online adaptation: as parameters evolve (and the random seed changes), we can continuously generate fresh samples that reflect the newly updated policy.

However, the main drawback of single-path estimation is variance: if each λ_k (and Z_k) is used only once, gradient estimates can fluctuate significantly, motivating larger batch sizes or smoothing techniques. In subsequent sections, we discuss strategies for mitigating this variance, including the alignment penalty (Section 5.3), which helps stabilize updates. Next, we detail how this single-path approach integrates into our discrete-time algorithm for computing $\nabla_{\theta} J$ and $\nabla_{\phi} J$ via BPTT, ultimately enabling a gradient-based update scheme for the policy parameters.

5.2 Discrete-Time Algorithm for Gradient Computation

We now present a concrete procedure, in discrete time, for computing both the adjoint processes (λ_t, Z_t) and the parameter gradients $(\nabla_{\theta} J, \nabla_{\phi} J)$. This algorithm relies on BPTT and handles both consumption and investment in the Merton problem.

- (a) **Discretize Dynamics and Objective.** Partition the interval $[0, T]$ into N steps of size $\Delta t = T/N$. Define $t_k = k\Delta t$ for $k = 0, \dots, N$, so that $t_0 = 0$ and $t_N = T$. We then approximate the SDE

$$dX_t = (rX_t + \pi_t(\mu - r)X_t - C_t) dt + \sigma\pi_t X_t dW_t$$

using Euler–Maruyama scheme:

$$X_{k+1} = X_k + (rX_k + \pi_k(\mu - r)X_k - C_k) \Delta t + \sigma\pi_k X_k \Delta W_k,$$

where $\pi_k = \pi_{\theta}(t_k, X_k)$, $C_k = C_{\phi}(t_k, X_k)$, and $\Delta W_k \sim \mathcal{N}(0, \Delta t)$. The continuous-time cost

$$J(\theta, \phi) = \mathbb{E} \left[\int_0^T e^{-\rho t} U(C_t) dt + \kappa e^{-\rho T} U(X_T) \right] \quad (19)$$

is discretized similarly as

$$J(\theta, \phi) \approx \mathbb{E} \left[\sum_{k=0}^{N-1} e^{-\rho t_k} U(C_k) \Delta t + \kappa e^{-\rho T} U(X_N) \right].$$

- (b) **Single Forward Path per (t_k, X_k) .** At each node (t_k, X_k) , we run exactly one forward simulation up to the terminal time T . This yields a single-sample payoff, which is noisy but unbiased. Using backpropagation afterward gives us an estimate of λ_k and Z_k under the current parameters (θ, ϕ) .

- (c) **Compute λ_k via BPTT.** In a typical deep-learning framework (e.g., PyTorch), we build a computational graph from (θ, ϕ) through $\{\pi_k, C_k\}$ and $\{X_k\}$ to $J(\theta, \phi)$. A single call to `.backward()` gives $\nabla_{\theta} J$ and $\nabla_{\phi} J$, as well as partial derivatives of J with respect to each X_k . Identifying $\lambda_k = \frac{\partial J}{\partial X_k}$ is consistent with the Pontryagin interpretation of an adjoint process.
- (d) **Obtain $\partial_x \lambda_k$ and Hence Z_k .** To compute Z_k , we need $\partial_x \lambda_k$. In practice, one applies another backward pass or higher-order autodiff on λ_k . Recalling that

$$Z_k = \sigma \pi_k X_k (\partial_x \lambda_k),$$

we emphasize this step does not impose optimality, but provides the extra derivative crucial for forming $\nabla_{\theta} J$ below.

- (e) **Update Network Parameters.** We collect the gradients with respect to θ and ϕ using, for instance:

$$\nabla_{\theta} J \approx \mathbb{E} \left[\sum_{k=0}^{N-1} \left(\lambda_k (\mu - r) X_k + Z_k \sigma X_k \right) \frac{\partial \pi_{\theta}(t_k, X_k)}{\partial \theta} \Delta t \right], \quad (20)$$

$$\nabla_{\phi} J \approx \mathbb{E} \left[\sum_{k=0}^{N-1} \left(-\lambda_k + e^{-\rho t_k} U'(C_k) \right) \frac{\partial C_{\phi}(t_k, X_k)}{\partial \phi} \Delta t \right]. \quad (21)$$

We then update (θ, ϕ) via a stochastic optimizer (e.g., Adam or SGD), iterating until the policy converges to a stationary solution of J .

In the formulas (20) and (21), the expectation $\mathbb{E}[\dots]$ is computed by sampling M trajectories (or mini-batches) and taking an empirical average:

$$\mathbb{E}[\dots] \approx \frac{1}{M} \sum_{i=1}^M [\dots]_i.$$

This algorithm effectively performs BPTT on a discretized Merton problem, using a single-path approach at each node (t_k, X_k) . Although variance can be large for any single sample, it remains unbiased in expectation. Repeated iteration gradually refines a Pontryagin-aligned policy, as each gradient step exploits the adjoint process (λ_k, Z_k) .

In practice, one could simply define π_{θ} and C_{ϕ} , compute $J(\theta, \phi)$ on sampled trajectories, call `.backward()`, and let autodiff produce $(\nabla_{\theta} J, \nabla_{\phi} J)$ in a black-box manner, without explicitly extracting λ_k or $\partial_x \lambda_k$. Nevertheless, interpreting (λ_k, Z_k) as suboptimal adjoint processes offers deeper insight and facilitates techniques like the alignment penalty in the next subsection that explicitly depend on $(\lambda_k, \partial_x \lambda_k)$.

5.3 Adjoint-Based Regularization for Pontryagin Alignment

Previously, we discussed how to obtain online estimates of λ_k and $\partial_x \lambda_k$ and thus derive the Pontryagin-optimal consumption and investment at each time step. In the Merton problem, for example, one obtains

$$C^{\text{PMP}}(t_k, X_k) = (e^{\rho t_k} \lambda_k)^{-\frac{1}{\gamma}}, \quad \pi^{\text{PMP}}(t_k, X_k) = -\frac{\mu - r}{\sigma^2 X_k} \times \frac{\lambda_k}{\partial_x \lambda_k} \quad (22)$$

from (8) and (9), where $\lambda_k = \lambda(t_k, X_k)$ and $\partial_x \lambda_k = \partial_x \lambda(t_k, X_k)$. These formulas reflect Pontryagin’s first-order conditions under CRRA utility.

However, the neural-network-based policies π_θ and C_ϕ may deviate from these ideal controls. A straightforward way to nudge the networks closer is to add an alignment penalty that measuring how far the learned policy is from $(C^{\text{PMP}}, \pi^{\text{PMP}})$. Specifically, we define

$$\mathcal{L}_{\text{align}}(\theta, \phi) = \beta_C \sum_k |C_\phi(t_k, X_k) - C^{\text{PMP}}(t_k, X_k)| + \beta_\pi \sum_k |\pi_\theta(t_k, X_k) - \pi^{\text{PMP}}(t_k, X_k)|, \quad (23)$$

where $\beta_C, \beta_\pi > 0$ control relative penalty on consumption versus investment mismatch, and the sums run over sampled nodes (t_k, X_k) . Each term penalizes how far the policy strays from the Pontryagin-based target.

Next, we augment the original objective $J(\theta, \phi)$ by defining

$$\tilde{J}(\theta, \phi) = J(\theta, \phi) - \mathcal{L}_{\text{align}}(\theta, \phi),$$

whose gradient combines the usual utility-maximization terms with additional component pushing (C_ϕ, π_θ) toward $(C^{\text{PMP}}, \pi^{\text{PMP}})$. Symbolically,

$$\nabla_{(\theta, \phi)} \tilde{J}(\theta, \phi) = \nabla_{(\theta, \phi)} \left(J(\theta, \phi) - \mathcal{L}_{\text{align}}(\theta, \phi) \right)$$

By choosing β_C and β_π , one can balance how much to penalize consumption versus investment mismatch. Moderate settings for both encourage Pontryagin-like policies without sacrificing the neural network’s expressive power, whereas larger values enforce stricter adherence to the analytical optimum but can slow or complicate convergence.

We opt for a soft regularization that gently steers the network toward locally optimal controls at each iteration. This design preserves flexibility, allowing the policy to adapt dynamically while leveraging Pontryagin’s insights to reduce drifting in high-dimensional parameter spaces. Such a strategy parallels other research that embeds theoretical knowledge via a penalty term rather than a hard constraint. For example, physics-informed neural networks (PINNs) (Raissi et al.,

2019) incorporate PDE residuals into the loss; PDE-constrained optimization applies adjoint information with soft constraints (Gunzburger, 2002; Hinze et al., 2008); and RL methods may regularize against an expert policy (Ross et al., 2011). As in these examples, our aim is to retain neural-network adaptability while preventing excessive deviation from known (or partially known) solutions.

5.4 Extended Value Function and Algorithmic Variants

5.4.1 Extended Value Function and Discretized Rollouts

In Section 5.2, we introduced a discretization scheme for the Merton problem over a fixed interval $[0, T]$. Here, we extend that approach to handle any initial time t_0 and wealth x_0 by defining an extended value function over a broader domain.

Many continuous-time problems (including Merton) require a policy (π_θ, C_ϕ) valid for any initial condition (t_0, x_0) . To address this requirement, we define an extended value function that integrates over random initial nodes $(t_0, x_0) \sim \eta(\cdot)$ in the domain $\mathcal{D} \subset [0, T] \times (0, \infty)$, and then discretize each resulting trajectory. Here, η denotes the distribution of (t_0, x_0) . Concretely, we set

$$\widehat{J}(\theta, \phi) = \mathbb{E}_{(t_0, x_0) \sim \eta} \left[\mathbb{E} \left(\int_{t_0}^T e^{-\rho u} U(C_\phi(u, X_u)) du + \kappa e^{-\rho T} U(X_T) \right) \right].$$

Hence, maximizing $\widehat{J}(\theta, \phi)$ yields a policy (π_θ, C_ϕ) that applies across all sub-intervals $[t_0, T]$ and initial wealth x_0 .

To avoid overfitting to a single initial scenario, we draw (t_0, x_0) from a suitable distribution η . By doing so, the policy (π_θ, C_ϕ) is trained to handle a broad region of the time–wealth domain rather than just one initial condition. This sampling strategy is standard in many PDE-based or RL-like continuous-time methods that need a single control law (π_θ, C_ϕ) covering all (t, x) .

To implement the integral in $\widehat{J}(\theta, \phi)$, one can follow the step-by-step procedure outlined in Algorithm 1, which details how to discretize the interval, simulate each path, and apply backpropagation to update (θ, ϕ) .

5.4.2 Gradient-Based Algorithmic Variants

Having introduced the extended value function over random initial nodes (t_0, x_0) , we now propose two core Pontryagin-Guided DPO (PG-DPO) algorithms for the Merton problem. Although both methods share the same extended-value rollout, they differ in whether they include a Pontryagin alignment penalty, and thus whether they require an additional autodiff pass to retrieve λ_0 and $\partial_x \lambda_0$.

(a) **PG-DPO (No Alignment Penalty).**

This is the baseline scheme (Algorithm 1), which simply maximizes $\widehat{J}(\theta, \phi)$ without regularization. A single BPTT pass suffices to obtain the approximate gradient $\nabla_{\theta}\widehat{J}, \nabla_{\phi}\widehat{J}$, and we update (θ, ϕ) until convergence. In classical Merton problems with strictly concave utility, any stationary point in continuous time is the unique global optimum, although non-convexities in the neural parameter space may introduce local minima. Empirically, PG-DPO typically converges near the known Pontryagin solution, but might exhibit slower or noisier training.

(b) **PG-DPO-Align (With Alignment Penalty).**

This extended scheme (Algorithm 2) incorporates the alignment penalty $\mathcal{L}_{\text{align}}$ to keep (π_{θ}, C_{ϕ}) near Pontryagin-optimal solution $(\pi^{\text{PMP}}, C^{\text{PMP}})$ in (22). We thus require a second BPTT (autodiff) pass to extract $\lambda_0 = \partial J / \partial X_0$ and $\partial_x \lambda_0$, from which we compute

$$\begin{aligned} C_0^{\text{PMP}} &:= C^{\text{PMP}}(t_0, X_0) = (e^{\rho t_0} \lambda_0)^{-\frac{1}{\gamma}}, \\ \pi_0^{\text{PMP}} &:= \pi^{\text{PMP}}(t_0, X_0) = -\frac{\mu - r}{\sigma^2 X_0} \times \frac{\lambda_0}{\partial_x \lambda_0}. \end{aligned}$$

We then form the augmented objective

$$\widehat{J}_{\text{align}}(\theta, \phi) = \widehat{J}(\theta, \phi) - \beta_C |C_{\phi}(t_0, X_0) - C_0^{\text{PMP}}| + \beta_{\pi} |\pi_{\theta}(t_0, X_0) - \pi_0^{\text{PMP}}|,$$

and update (θ, ϕ) to maximize $\widehat{J}_{\text{align}}$. This alignment step can often yield more stable or faster convergence (though at higher computational cost).

Note that both PG-DPO and PG-DPO-Align extend naturally to random initial nodes (t_0, x_0) , enabling the learned policy to cover the entire domain of interest. Moreover, we need only λ_0 (rather than the entire $\{\lambda_k\}_{k=0}^N$) in Algorithm 2, because we choose X_0 (the initial wealth) from a distribution that covers the relevant domain of X_t , so performing BPTT solely with respect to X_0 suffices. Thus, automatic differentiation with respect to X_0 internally accounts for how $\{X_k\}_{k=1}^N$ evolve, and we can directly obtain

$$\lambda_0 = \frac{\partial J}{\partial X_0}, \quad \partial_x \lambda_0 = \frac{\partial^2 J}{\partial X_0^2},$$

which allow us to compute π_0^{PMP} and C_0^{PMP} for the alignment penalty. Consequently, this saves memory, simplifies the code, and still provides a rich set of λ_0 estimates across the domain.

Algorithm 1 PG-DPO (No Alignment Penalty)

Inputs:

- Policy nets (π_θ, C_ϕ)
- Step sizes $\{\alpha_k\}$, total iterations K
- Domain sampler for $(t_0^{(i)}, x_0^{(i)})$ over $\mathcal{D} \subset [0, T] \times (0, \infty)$
- Fixed integer N (number of time steps per path)

1: **for** $j = 1$ to K **do**

2: **(a) Sample mini-batch of size M :** For each $i \in \{1, \dots, M\}$, draw initial $(t_0^{(i)}, x_0^{(i)})$ from \mathcal{D} .

3: **(b) Local Single-Path Simulation for each i :**

(a) *Define local step:* $\Delta t^{(i)} \leftarrow \frac{T-t_0^{(i)}}{N}$, $t_0^{(i)} < t_1^{(i)} < \dots < t_N^{(i)} = T$, with $t_k^{(i)} = t_0^{(i)} + k \Delta t^{(i)}$.

(b) *Initialize wealth:* $X_0^{(i)} \leftarrow x_0^{(i)}$.

(c) *Euler–Maruyama:* For $k = 0, \dots, N - 1$:

$$X_{k+1}^{(i)} = X_k^{(i)} + \left[r X_k^{(i)} + \pi_\theta(t_k^{(i)}, X_k^{(i)}) (\mu - r) X_k^{(i)} - C_\phi(t_k^{(i)}, X_k^{(i)}) \right] \Delta t^{(i)} \\ + \sigma \pi_\theta(t_k^{(i)}, X_k^{(i)}) X_k^{(i)} \Delta W_k^{(i)}.$$

where $\Delta W_k^{(i)} \sim \mathcal{N}(0, \Delta t^{(i)})$.

(d) *Local cost:*

$$J^{(i)}(\theta, \phi) = \sum_{k=0}^{N-1} e^{-\rho t_k^{(i)}} U\left(C_\phi(t_k^{(i)}, X_k^{(i)})\right) \Delta t^{(i)} + \kappa e^{-\rho T} U(X_N^{(i)}).$$

4: **(c) Backprop (single pass) & Averaging:**

$$\widehat{J}(\theta, \phi) = \frac{1}{M} \sum_{i=1}^M J^{(i)}(\theta, \phi), \quad \nabla_{(\theta, \phi)} \widehat{J} \leftarrow \text{BPTT on each } J^{(i)}.$$

5: **(d) Parameter Update:**

$$\theta \leftarrow \theta + \alpha_k \nabla_\theta \widehat{J}, \quad \phi \leftarrow \phi + \alpha_k \nabla_\phi \widehat{J}.$$

6: **end for**

7: **return** Final policy (π_θ, C_ϕ) .

Algorithm 2 PG-DPO-Align (With Alignment Penalty)

Additional Inputs:

- Alignment weights (α_C, α_π) ;
- Suboptimal adjoint $(\lambda_0^{(i)}, \partial_x \lambda_0^{(i)})$ from a second BPTT pass.

1: **for** $j = 1$ to K **do**

2: **(a) Domain Sampling & Single-Path Simulation:** As in PG-DPO, collect each $J^{(i)}(\theta, \phi)$.

3: **(b) Retrieve Adjoint Info (2nd pass):**

 i) For each path i , run extra autodiff to get $\lambda_0^{(i)} = \frac{\partial J^{(i)}}{\partial X_0^{(i)}}$ and $\partial_x \lambda_0^{(i)}$.

 ii) Pontryagin controls:

$$C_0^{\text{PMP},(i)} = (e^{\rho t_0} \lambda_0^{(i)})^{-\frac{1}{\gamma}}, \quad \pi_0^{\text{PMP},(i)} = -\frac{\mu - r}{\sigma^2 X_0^{(i)}} \frac{\lambda_0^{(i)}}{\partial_x \lambda_0^{(i)}}.$$

4: **(c) Full Objective with Alignment Penalty:**

$$\begin{aligned} \widehat{J}_{\text{align}}(\theta, \phi) = \frac{1}{M} \sum_{i=1}^M & \left[J^{(i)}(\theta, \phi) - \beta_C \left| C_\phi^{(i)}(t_0, X_0) - C_0^{\text{PMP},(i)} \right| \right. \\ & \left. + \beta_\pi \left| \pi_\theta^{(i)}(t_0, X_0) - \pi_0^{\text{PMP},(i)} \right| \right] \end{aligned}$$

5: **(d) : BPTT & Update:**

$\nabla_\theta \widehat{J}_{\text{align}}, \nabla_\phi \widehat{J}_{\text{align}} \leftarrow$ BPTT on each term.

$\theta \leftarrow \theta + \alpha_0 \nabla_\theta \widehat{J}_{\text{align}}, \quad \phi \leftarrow \phi + \alpha_0 \nabla_\phi \widehat{J}_{\text{align}}.$

6: **end for**

7: **return** Final policy (π_θ, C_ϕ) balancing \widehat{J} and alignment penalty.

6 Stochastic Approximation and Convergence Analysis

In this section, we establish a self-contained convergence result for our stochastic approximation scheme and then extend it to the augmented objective that includes the alignment penalty from Section 5.3. Both arguments build on classical Robbins–Monro theory, ensuring that, under standard assumptions, our gradient-based updates converge almost surely to a stationary point.

6.1 Convergence Analysis for the Baseline Objective $J(\theta, \phi)$

We begin with the baseline problem of maximizing $J(\theta, \phi)$ in (19), where (θ, ϕ) parametrize the policy networks π_θ and C_ϕ . In practice, as discussed in Section 5.2, the continuous-time Merton objective is discretized by a time-step $\Delta t = T/N$ and approximated by a mini-batch or single-path sampling scheme, thus yielding gradient estimates $\hat{g}_k(\theta, \phi)$. Strictly speaking, when $\Delta t > 0$ is finite, a small residual discretization bias may remain. However, as $\Delta t \rightarrow 0$, this bias diminishes, and under a well-designed mini-batch sampling, \hat{g}_k is regarded as an unbiased (or nearly unbiased) estimator of ∇J .

Key Assumptions (cf. Kushner & Yin, 2003; Borkar & Borkar, 2008)

(A1) (Lipschitz Gradients) The mapping $\nabla J(\theta, \phi)$ is globally Lipschitz on a compact domain $\Theta \times \Phi$. That is, there exists some constant $L_J > 0$ such that

$$\|\nabla J(\theta, \phi) - \nabla J(\theta', \phi')\| \leq L_J \|(\theta, \phi) - (\theta', \phi')\|$$

for all (θ, ϕ) and (θ', ϕ') in $\Theta \times \Phi$.

(A2) (Unbiased, Bounded-Variance Gradients) For each iteration k , the gradient estimate $\hat{g}_k(\theta, \phi)$ satisfies

$$\mathbb{E}[\hat{g}_k(\theta, \phi)] = \nabla J(\theta, \phi) + \delta_k, \quad \mathbb{E}[\|\hat{g}_k(\theta, \phi)\|^2] \leq B,$$

where $\|\delta_k\| \rightarrow 0$ as $\Delta t \rightarrow 0$ (eliminating discretization bias). In typical mini-batch SGD, \hat{g}_k is unbiased at each iteration (assuming i.i.d. sampling from the underlying distribution), and the variance is uniformly bounded by $B > 0$.

(A3) (Robbins–Monro Step Sizes) The step sizes $\{\alpha_k\}$ satisfy

$$\sum_{k=0}^{\infty} \alpha_k = \infty, \quad \sum_{k=0}^{\infty} \alpha_k^2 < \infty.$$

This ensures a standard Robbins–Monro (stochastic gradient) iteration.

Under these assumptions, our parameter update is

$$(\theta_{k+1}, \phi_{k+1}) = (\theta_k, \phi_k) + \alpha_k \hat{g}_k(\theta_k, \phi_k),$$

where the term δ_k (if any) shrinks as $\Delta t \rightarrow 0$.

Theorem 1 (Baseline Robbins–Monro Convergence). *Suppose (A1)–(A3) hold, and that $\|\delta_k\| \rightarrow 0$ as $\Delta t \rightarrow 0$. Then, with probability one,*

$$(\theta_k, \phi_k) \xrightarrow[k \rightarrow \infty]{a.s.} (\theta^\dagger, \phi^\dagger),$$

where $\nabla J(\theta^\dagger, \phi^\dagger) = 0$. In other words, $(\theta^\dagger, \phi^\dagger)$ is a stationary point of J in the parameter space.

Proof Sketch. As $\Delta t \rightarrow 0$, each $\hat{g}_k(\theta, \phi)$ becomes (approximately) unbiased with bounded variance. By the classical Robbins–Monro argument (Kushner & Yin, 2003; Borkar & Borkar, 2008), the iterates (θ_k, ϕ_k) converge almost surely to a point where $\nabla J = 0$. \square

This result ensures that our parameter sequence converges to a stationary point in the parameter space (θ, ϕ) . However, because π_θ and C_ϕ are encoded by neural networks, the objective surface can be non-convex (Choromanska et al., 2015; Goodfellow, 2016), potentially admitting multiple local optima. Meanwhile, in classical Merton settings with strictly concave utility, the continuous-time control space (π_t, C_t) has a unique global optimum for the original objective. Empirically, we observe that for typical Merton parameters (e.g., CRRA utility), the learned neural policy aligns closely with this global solution, indicating that even though the parametric surface is non-convex, the algorithm tends to find a near-global optimum in practice.

6.2 Convergence Analysis for the Augmented Objective $\tilde{J}(\theta, \phi)$

We now show that introducing the adjoint-based regularization term (Section 5.3) does not invalidate the convergence guarantees established in Section 6.1. Recall the augmented objective:

$$\tilde{J}(\theta, \phi) = J(\theta, \phi) - \mathcal{L}_{\text{align}}(\theta, \phi),$$

where $\mathcal{L}_{\text{align}}$ penalizes deviations from Pontryagin-derived controls $(\pi^{\text{PMP}}, C^{\text{PMP}})$. In classical Merton settings with strictly concave utility, the global optimum of J

also makes $\mathcal{L}_{\text{align}}$ vanish (i.e., no deviation from the Pontryagin solution), so \tilde{J} and J share the same unique global maximizer in the continuous-time sense.

Formally, we have

$$\nabla_{(\theta, \phi)} \tilde{J}(\theta, \phi) = \nabla_{(\theta, \phi)} J(\theta, \phi) - \nabla_{(\theta, \phi)} \mathcal{L}_{\text{align}}(\theta, \phi). \quad (24)$$

Key Assumptions for the Augmented Objective. As before, let $\hat{g}_k(\theta, \phi)$ be an (approximately) unbiased, bounded-variance estimator of $\nabla J(\theta, \phi)$, as in (A2). Now define $\hat{h}_k(\theta, \phi)$ analogously as an (approximately) unbiased, bounded-variance estimator of $\nabla \mathcal{L}_{\text{align}}(\theta, \phi)$. For convenience, we label the assumptions for \tilde{J} as (B1)–(B3), mirroring those of (A1)–(A3):

(B1) (Lipschitz Gradients for \tilde{J}) Suppose $\nabla \mathcal{L}_{\text{align}}$ is Lipschitz on the same compact domain $\Theta \times \Phi$. In particular, if π_θ and C_ϕ each lie in a bounded set with bounded derivatives, then $\nabla \mathcal{L}_{\text{align}}$ is Lipschitz. Combined with (A1), it follows that $\nabla \tilde{J}$ is also globally Lipschitz.

(B2) (Approximately Unbiased, Bounded-Variance Gradients for \tilde{J}) We define

$$\hat{f}_k(\theta, \phi) = \hat{g}_k(\theta, \phi) - \hat{h}_k(\theta, \phi),$$

mirroring (24). As in (A2), each of \hat{g}_k and \hat{h}_k may exhibit a small bias term δ_k that vanishes as $\Delta t \rightarrow 0$. Hence, \hat{f}_k is effectively an unbiased estimator of $\nabla \tilde{J}$ with uniformly bounded variance (by some constant $\tilde{B} > 0$) in the limit of fine discretization.

(B3) (Robbins–Monro Step Sizes) The step sizes $\{\alpha_k\}$ again satisfy

$$\sum_{k=0}^{\infty} \alpha_k = \infty, \quad \sum_{k=0}^{\infty} \alpha_k^2 < \infty.$$

This ensures a standard Robbins–Monro iteration for \tilde{J} .

Under these assumptions, the parameter update is

$$(\theta_{k+1}, \phi_{k+1}) = (\theta_k, \phi_k) + \alpha_k \hat{f}_k(\theta_k, \phi_k).$$

Theorem 2 (Stationarity of \tilde{J}). *Suppose (B1)–(B3) hold. Then, with probability one,*

$$(\theta_k, \phi_k) \xrightarrow[k \rightarrow \infty]{a.s.} (\theta^\dagger, \phi^\dagger),$$

where $\nabla \tilde{J}(\theta^\dagger, \phi^\dagger) = 0$. In other words, $(\theta^\dagger, \phi^\dagger)$ is a stationary point of the augmented objective \tilde{J} .

Proof Sketch. By (B1), $\nabla \tilde{J}$ is Lipschitz (as it is the sum/difference of Lipschitz functions). By (B2), \hat{f}_k is (approximately) unbiased with uniformly bounded variance in the limit of $\Delta t \rightarrow 0$. By (B3), the step sizes satisfy Robbins–Monro conditions. Hence, the argument from Theorem 1 applies again, guaranteeing that (θ_k, ϕ_k) converges almost surely to a point where $\nabla \tilde{J} = 0$. \square

Theorem 2 establishes that even after adding the alignment penalty $\mathcal{L}_{\text{align}}$, the updated scheme converges (a.s.) to a stationary point of \tilde{J} . Intuitively, this reflects a balance between maximizing the original Merton objective J and staying near the Pontryagin-based controls. In highly non-convex neural-network models, multiple such stationary points may exist, so the algorithm may converge to one of them in the parameter space. However, in classical Merton settings with strictly concave utility, there is a unique global optimum in continuous time that makes $\mathcal{L}_{\text{align}}$ vanish. The presence of this penalty typically helps steer the finite-dimensional parameter updates more reliably toward that unique global maximizer, thus boosting numerical stability. Overall, adding $\mathcal{L}_{\text{align}}$ neither disrupts the baseline convergence nor alters the fundamental optimum in strictly concave Merton scenarios.

7 Numerical Results

In this section, we demonstrate our Pontryagin-guided neural approach on the Merton problem with both consumption and investment, distinguishing it from prior works that focus primarily on investment decisions (e.g., Reppen et al., 2023; Reppen & Soner, 2023; Dai et al., 2023). Incorporating consumption notably increases the dimensionality and difficulty for classical PDE/finite-difference methods.

We consider a one-year horizon $T = 1$ and restrict the wealth (state) domain to $[0.1, 2]$. The model parameters are $r = 0.03$, $\mu = 0.12$, $\sigma = 0.2$, $\varepsilon = 0.1$, $\gamma = 2$, and $\rho = 0.02$. Two neural networks C_ϕ and π_θ approximate the consumption and portfolio policies, respectively, each taking (t, X_t) as input so that the entire state-time domain is handled by a single pipeline without needing to stitch local solutions. Both nets have two hidden layers (200 nodes each) with Leaky-ReLU activation. We draw 10,000 initial samples (t, X_t) uniformly in the time-wealth domain $\mathcal{D} = [0, 1] \times [0.1, 2]$. At each iteration, a fresh batch is simulated in real time via Euler–Maruyama to prevent overfitting to a single dataset and to ensure the policy remains adapted to the evolving environment.

We compare two variants of our scheme:

- (a) **PG-DPO:** This is the baseline algorithm (Algorithm 1), which uses the discrete-time gradient-based updates from Section 5.2 without adding a Pontryagin alignment term.

Table 1: **PG-DPO** vs. **PG-DPO-Align** in the Merton problem. We compare relative MSEs (consumption/investment) and empirical utility at various iteration milestones. PG-DPO uses step sizes of 1×10^{-3} (investment) and 1×10^{-5} (consumption), while PG-DPO-Align includes an alignment penalty $\mathcal{L}_{\text{align}}$ with $(\beta_C, \beta_\pi) = (10^{-3}, 10^{-1})$ chosen after brief tuning.

Iterations		1,000	10,000	50,000	100,000
Rel. MSE (Consumption)	PG-DPO	3.14e+00	5.73e-01	1.39e-01	9.65e-02
	PG-DPO-Align	3.00e+00	3.75e-01	6.25e-02	3.46e-02
Rel. MSE (Investment)	PG-DPO	2.39e-02	2.13e-02	7.85e-03	1.19e-02
	PG-DPO-Align	7.22e-02	1.57e-02	9.82e-03	8.43e-03
Empirical Utility	PG-DPO	6.5420e-01	6.4795e-01	6.4791e-01	6.4791e-01
	PG-DPO-Align	6.5434e-01	6.4793e-01	6.4791e-01	6.4791e-01

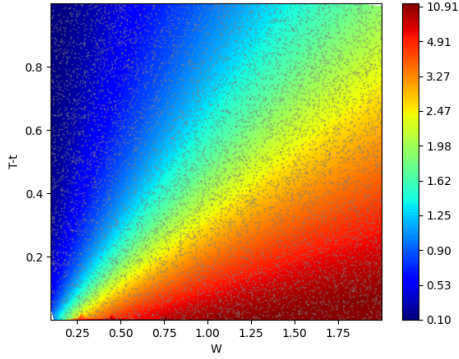
- (b) **PG-DPO-Align**: This variant adds the penalty $\mathcal{L}_{\text{align}}$ (cf. Section 5.3). After brief tuning, we set $(\beta_C, \beta_\pi) = (10^{-3}, 10^{-1})$, noting that too large a penalty can slow early training, while too small a penalty yields minimal improvement. We also allow for different learning rates for the two policy networks: 1×10^{-5} for consumption, 1×10^{-3} for investment.

Both methods are trained with the Adam optimizer for up to 100,000 iterations. At intermediate checkpoints (1k, 10k, 50k, 100k), we measure: (1) the relative mean-squared error (MSE) between the learned policy and the known closed-form solution, (2) an empirical utility obtained by averaging the realized payoffs over 500 rollouts centered around that iteration, to gauge practical performance.

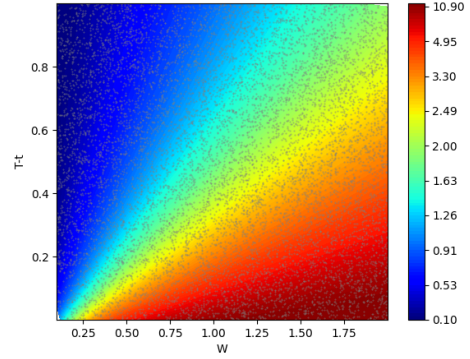
Table 1 summarizes the relevant error metrics and empirical utility outcomes. From this table, we observe that **PG-DPO-Align** often converges more stably or quickly, especially at high iteration counts.

Figure 1 then compares the learned policies (after 100k iterations of PG-DPO-Align) to the known closed-form Merton solution. Despite the additional difficulty from incorporating consumption, the proposed method converges closely to the theoretical optimum.

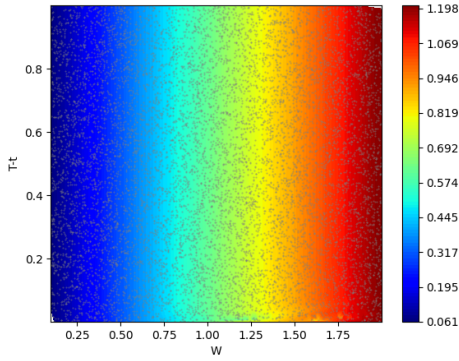
In general, both **PG-DPO** and **PG-DPO-Align** eventually reach high utility levels, with empirical utility converging near the theoretical maximum. However, **PG-DPO-Align** yields lower MSE for both consumption and investment at higher iteration counts (e.g., 3.46×10^{-2} vs. 9.65×10^{-2} in consumption MSE at 100k steps), suggesting that the alignment penalty guides the policy more effectively toward Pontryagin solutions. We also observe that the alignment variant often



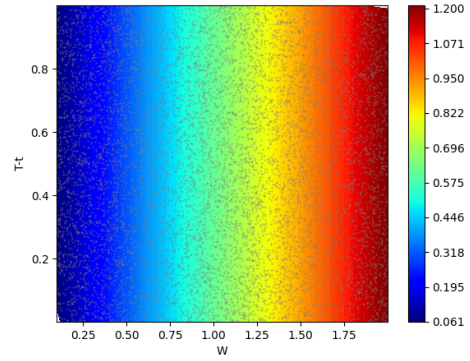
(a) Learned consumption policy



(b) Exact consumption formula



(c) Learned investment policy



(d) Exact investment formula

Figure 1: Neural vs. exact solutions for consumption/investment under the Merton model. The learned plots (left) are from our **PG-DPO-Align** run at iteration 100,000; the exact plots (right) show the closed-form Merton solution.

stabilizes faster, though the penalty weights (β_C, β_π) must be set moderately to avoid slowing early progress.

Overall, these results confirm that a Pontryagin-guided alignment approach can improve both stability and final accuracy in learning the Merton policy. While the naive gradient method (PG-DPO) ultimately reaches comparable utility, PG-DPO-Align leverages the local Pontryagin reference at each step, thereby achieving better performance in practice and more faithfully matching the known closed-form solution.

8 Conclusion

We have proposed a PG-DPO framework for Merton’s portfolio problem (Section 5), combining neural-network-based gradient methods with the adjoint perspective from PMP. By parametrizing both consumption and investment policies within neural networks and aligning each gradient step to approximate the continuous-time adjoint, our approach balances theoretical rigor with practical flexibility.

A central design choice is to handle the entire time–wealth domain by defining an extended value function over random initial nodes (t_0, x_0) . This domain-aware sampling allows the policy to learn a truly global solution rather than overfitting to a single initial state. After discretizing only the local sub-interval from t_0 to T , we apply single-path or mini-batch simulation to obtain unbiased gradient estimates, ensuring that the learned policy covers a broad region of $[0, T] \times (0, \infty)$.

In addition, we introduce an adjoint-based alignment penalty that softly regularizes the policy toward Pontryagin’s local controls. Numerical experiments confirm that including this penalty can substantially improve stability and reduce final policy errors, despite the extra cost of a second autodiff pass to retrieve the suboptimal adjoint processes λ_t and $\partial_x \lambda_t$. Our results on the Merton problem with consumption show that the alignment-penalty variant (PG-DPO-Align) outperforms the basic scheme (PG-DPO) in terms of convergence speed and accuracy, while both ultimately reach near-optimal empirical utilities.

Although we do not guarantee global optimality in the high-dimensional neural parameter space, the strict concavity of the Merton objective ensures a unique global optimum in continuous time. Empirically, the extended domain and alignment penalty help guide parameter updates more reliably toward this Pontryagin-aligned solution, even in the presence of non-convexities.

Moreover, to the best of our knowledge, no existing deep-BSDE or PINN approach addressing Merton’s problem with both consumption and investment in a single framework. By offering a Pontryagin-based perspective, our PG-DPO method fills this gap and further demonstrates how continuous-time control principles can enrich modern deep learning approaches to stochastic optimization.

Further refinements could explore advanced variance-reduction techniques, expand to higher-dimensional or constrained markets, or combine value-based PDE elements with the adjoint-based insights. Overall, these findings illustrate how continuous-time control principles can enrich modern deep learning approaches to stochastic optimization. By embedding the local costate viewpoint into a discrete-time training loop, the PG-DPO framework provides an efficient path to near-optimal controls for complex continuous-time finance problems and beyond.

Acknowledgments

Jeonggyu Huh received financial support from the National Research Foundation of Korea (Grant No. NRF-2022R1F1A1063371). This work was supported by the National Research Foundation of Korea (NRF) grant funded by the Korea government (MSIT) (RS-2024-00355646).

References

- Beck, C., E, W., & Jentzen, A. (2019). Machine learning approximation algorithms for high-dimensional fully nonlinear partial differential equations and second-order backward stochastic differential equations. *Journal of Nonlinear Science*, 29, 1563–1619. 1
- Becker, S., Cheridito, P., & Jentzen, A. (2019). Deep optimal stopping. *Journal of Machine Learning Research*, 20(74), 1–25. 1
- Borkar, V. S. & Borkar, V. S. (2008). *Stochastic approximation: a dynamical systems viewpoint*, volume 9. Springer. 5.1, 6.1, 6.1
- Buehler, H., Gonon, L., Teichmann, J., & Wood, B. (2019). Deep hedging. *Quantitative Finance*, 19(8), 1271–1291. 1
- Choromanska, A., Henaff, M., Mathieu, M., Arous, G. B., & LeCun, Y. (2015). The loss surfaces of multilayer networks. In *Artificial intelligence and statistics* (pp. 192–204).: PMLR. 6.1
- Dai, M., Dong, Y., Jia, Y., & Zhou, X. Y. (2023). Learning merton’s strategies in an incomplete market: Recursive entropy regularization and biased gaussian exploration. *arXiv preprint arXiv:2312.11797*. 1, 7
- Fleming, W. H. & Soner, H. M. (2006). *Controlled Markov processes and viscosity solutions*, volume 25. Springer Science & Business Media. 3.1, 3.1, 4.2
- Goodfellow, I. (2016). Deep learning. 6.1
- Gunzburger, M. D. (2002). *Perspectives in flow control and optimization*. SIAM. 5.3
- Han, J. & E, W. (2016). Deep learning approximation for stochastic control problems. *arXiv preprint arXiv:1611.07422*. 1

- Han, J., Jentzen, A., & E, W. (2018). Solving high-dimensional partial differential equations using deep learning. *Proceedings of the National Academy of Sciences*, 115(34), 8505–8510. 1, 4
- Hinze, M., Pinnau, R., Ulbrich, M., & Ulbrich, S. (2008). *Optimization with PDE constraints*, volume 23. Springer Science & Business Media. 5.3
- Huré, C., Pham, H., & Warin, X. (2020). Deep backward schemes for high-dimensional nonlinear pdes. *Mathematics of Computation*, 89(324), 1547–1579. 1, 4
- Karatzas, I. & Shreve, S. E. (1998). *Methods of Mathematical Finance*. New York: Springer. 1, 2
- Kushner, H. J. & Yin, G. G. (2003). *Stochastic Approximation and Recursive Algorithms and Applications*. New York: Springer Science & Business Media. 5.1, 6.1, 6.1
- Ma, J. & Yong, J. (1999). *Forward-backward stochastic differential equations and their applications*. Number 1702. Springer Science & Business Media. 3.2.3
- Merton, R. C. (1971). Optimum consumption and portfolio rules in a continuous-time model. *Journal of Economic Theory*, 3(4), 373–413. 1, 2
- Pardoux, E. & Peng, S. (1990). Adapted solution of a backward stochastic differential equation. *Systems & control letters*, 14(1), 55–61. 3.1, 3.2.3
- Pham, H. (2009). *Continuous-time stochastic control and optimization with financial applications*, volume 61. Springer Science & Business Media. 1, 3.1, 3.1
- Pontryagin, L. S. (2018). *Mathematical theory of optimal processes*. Routledge. 1, 3.1, 4.2
- Raissi, M., Perdikaris, P., & Karniadakis, G. E. (2019). Physics-informed neural networks: A deep learning framework for solving forward and inverse problems involving nonlinear partial differential equations. *Journal of Computational physics*, 378, 686–707. 5.3
- Reppen, A. M. & Soner, H. M. (2023). Deep empirical risk minimization in finance: Looking into the future. *Mathematical Finance*, 33(1), 116–145. 1, 7
- Reppen, A. M., Soner, H. M., & Tissot-Daguette, V. (2023). Deep stochastic optimization in finance. *Digital Finance*, 5(1), 91–111. 1, 7

- Ross, S., Gordon, G., & Bagnell, D. (2011). A reduction of imitation learning and structured prediction to no-regret online learning. In *Proceedings of the fourteenth international conference on artificial intelligence and statistics* (pp. 627–635).: JMLR Workshop and Conference Proceedings. 5.3
- Weinan, E. (2017). A proposal on machine learning via dynamical systems. *Communications in Mathematics and Statistics*, 1(5), 1–11. 1, 4
- Yong, J. & Zhou, X. Y. (2012). *Stochastic controls: Hamiltonian systems and HJB equations*, volume 43. Springer Science & Business Media. 1, 2, 3.1, 3.1, 3.2.3
- Zhang, W. & Zhou, C. (2019). Deep learning algorithm to solve portfolio management with proportional transaction cost. In *2019 IEEE Conference on Computational Intelligence for Financial Engineering & Economics (CIFER)* (pp. 1–10).: IEEE. 1